

# Echelle Diffractive Grating Based Wavelength Interrogator for Potential Aerospace Applications

Honglei Guo, Gaozhi Xiao, *Senior Member, IEEE*, Nezhir Mrad, and Jianping Yao, *Fellow, IEEE, Fellow, OSA*

**Abstract**—Operational load monitoring and impact damage detection are the two critical aspects of aerospace structural health monitoring (SHM). Fiber Bragg grating (FBG) sensors have demonstrated great potential in both. But the currently available interrogation systems can only handle one of the two types of SHM capabilities offered by FBG sensors. In addition, the practical implementation of FBG sensor systems in aerospace vehicles requires the interrogator to be small size, light weight, and low-power consuming. In this paper, we present an Echelle diffractive grating (EDG) based interrogation system for FBG sensors, which possesses two operation modes, i.e., the sweeping mode for operational load monitoring and the parked mode for impact damage detection. Experimental results show that this interrogator offers better than 1-pm measurement resolution and 10-pm repeatability. In addition, the interrogation system is very compact and weighs less than 60 g (excluding the electronic controller). It also has the potential to achieve a measurement speed of 300 kHz and be powered by a battery.

**Index Terms**—Echelle diffractive grating, fiber Bragg grating (FBG), fiber optic sensors, interrogator.

## I. INTRODUCTION

AEROSPACE structural health monitoring (SHM) has been an attractive topic of research for both academia and the industry for the past 20 years. It is aiming to improve the operational cost-effectiveness and reduce the maintenance cost [1]. Operational load monitoring and impact damage detection are the two critical aspects of aerospace SHM [2]. Operational load monitoring can be inferred from strain measurement and used to evaluate the structural status of aircrafts by comparing the measurand data to the designed structural performance [3]. Although this technique has been proven relatively mature for aerospace SHM applications, the load monitoring methods usually lack the high sensitivity required for damage location and quantification [2]. Therefore, a variety of other techniques have

been introduced and studied for the impact damage detection. Those are mainly based on an actuation-sensing process using ultrasonic/acoustic waves [4]. Currently, electrical strain gauge sensors are the most mature and developed solutions for operational load monitoring, and piezoelectric (PZT) based acoustic sensors are the most studied techniques for impact damage detection. However, all those sensors need their own dedicated wires and suffer from poor multiplexing capability, resulting in wiring challenges when multiple sensor deployment is required [5]. In addition, they are vulnerable to adverse interference such as electromagnetic interference (EMI), and need shields for the insulation [6].

On the other hand, tens and/or hundreds of fiber Bragg grating (FBG) sensors can be fabricated and multiplexed in a single optical fiber. FBG sensors are light weight, small size and immune to EMI. Thus, FBG sensors offer the potential to significantly alleviate the wiring challenges and EMI issue, making them particularly attractive for large-scale structural SHM applications [7], [8]. For aerospace SHM applications, FBG sensors can not only be used for either operational load monitoring (changes of strain) [9] or impact damage inspection (detection of acoustic signals) [10] respectively, but also offer the possibility in fulfilling the two tasks at the same time [11], which is regarded as an added advantage for FBG sensors. However, the lack of a suitable interrogation system hinders the use of FBG sensors from doing both the load monitoring and the damage detection. Currently available sensor interrogators can only perform one of the two SHM tasks. For operational load monitoring, it is required to measure large changes (thousands of  $\mu\epsilon$ ) at a low speed (static). While for impact damage detection, the capability of measuring acoustic signals, i.e., small changes (tens of  $\mu\epsilon$ ) at an ultrafast speed (50 kHz–500 kHz), is usually required for a standard FBG sensor with a 10-mm grating length [12]. Based on the classification of interrogation techniques by the speed as described in [13], tunable Fabry-Perot (FP) filter can be used when the interrogation speed required is under 1 kHz, and the combination of a diffractive grating and a CCD array is suitable for a speed from 1 kHz to 20 kHz [14]. For a speed from 20 kHz up to 500 kHz, three methods have been reported, i.e., the use of a laser diode with its output wavelength fixed at the middle of one FBG spectrum slope [10], an FP filter with its spectrum broadened and fixed [15], and an arrayed waveguide grating (AWG) with its spectrum fixed [16]. However, none of them is reported to have the capability of performing both tasks of load monitoring and damage detection as required by aerospace SHM.

To address this issue, we introduce an interrogator that operates in two operation modes, i.e., the sweeping mode and

Manuscript received January 09, 2013; revised March 22, 2013; accepted April 23, 2013. Date of publication May 15, 2013; date of current version May 31, 2013. This work was supported in part by the Canadian Institute for Photonics Innovations, National Research Council Canada and the Department of National Defence Canada.

H. Guo and J. Yao are with the Microwave Photonics Research Laboratory, School of Electrical Engineering and Computer Science, University of Ottawa, ON K1N 6N5, Canada.

G. Xiao is with the Institute for Microstructural Science, National Research Council Canada, Ottawa, ON K1A 0R6, Canada (e-mail: George.Xiao@nrc-cnrc.gc.ca).

N. Mrad is with the Centre for Security Science (CSS), Defence R&D Canada, Department of National Defence, National Defence Headquarters, Ottawa, ON K1A 0K2, Canada

Color versions of one or more of the figures in this paper are available online at <http://ieeexplore.ieee.org>.

Digital Object Identifier 10.1109/JLT.2013.2263278

the parked mode, to a miniaturized interrogation system previously developed. This system is based on a monolithically integrated Echelle diffractive grating (EDG) device [17], [18], which is fabricated by the planar lightwave circuit technology and with the features of small size, light weight, and strong reliability proved by the stringent telecommunication standards. The sweeping mode, in which the transmission wavelength of the EDG channel is tuned by adjusting the EDG chip temperature, can be used for the load monitoring, while the parked mode, in which the transmission wavelength of all the EDG channels is fixed, can be used for the damage detection. To the best of our knowledge, this is the first interrogator ever reported to offer the dual functions.

The paper is organized as follows. In Section II, we introduce the theory for the operation of this dual function interrogator. In Section III, we describe the experimental setup and present the test results. The characteristics of the dual function interrogator are discussed. A conclusion is drawn in Section IV.

## II. THEORY

In order to achieve the dual functions required, the previously developed EDG-based interrogator is modified, in which only the odd number EDG channels are connected in order to reduce the electronic complexity [17], [18]. In this design, all the 32 channels of the EDG, including the odd and even number EDG channels, are used with the EDG spectrum shown in Fig. 1. In the sweeping mode, the transmission wavelength of each EDG channel is tuned by changing the EDG temperature. The wavelength interrogation principle is the same as the one described in [17], [18]. By monitoring the light power and recording the EDG temperature, the EDG temperature corresponding to the peak light power could be found. With the proven linear relationship between the EDG transmission wavelength and its temperature, the Bragg wavelength of an FBG sensor can be accurately interrogated. The use of 32 channels makes the channel spacing be 0.8 nm instead of 1.6 nm used in the previous studies. Thus, the EDG temperature tuning range required to move one EDG transmission wavelength from one channel to its neighboring channel is reduced by half, resulting in a lower power consumption in the sweeping mode operation and an increase in the measurement repeatability. As demonstrated in our previous studies [18], this sweeping mode can be used for large strain variation, which is suitable for the interrogation of load monitoring FBG sensors.

Also, due to the reduction of the channel spacing from 1.6 nm to 0.8 nm, the two neighboring EDG channels have an overlapped region. This makes it possible for the interrogator to operate in the parked mode based on the principle described in [16], [19]. In this mode, the FBG sensors are interrogated by using a linear wavelength-dependent optical filter consisting of two adjacent EDG channels, as shown in Fig. 2. Only small variation of strain recorded by an FBG sensor can be accurately interrogated using this method, but at a very high speed. In [16], an interrogator based on an AWG reaches a speed up to 300 kHz, and is used to interrogate FBG acoustic sensors for aerospace damage detection. Our EDG device has the same spectrum profile as that of an AWG. Thus, it has the same interrogation capability of using a fixed spectrum in the parked mode for the

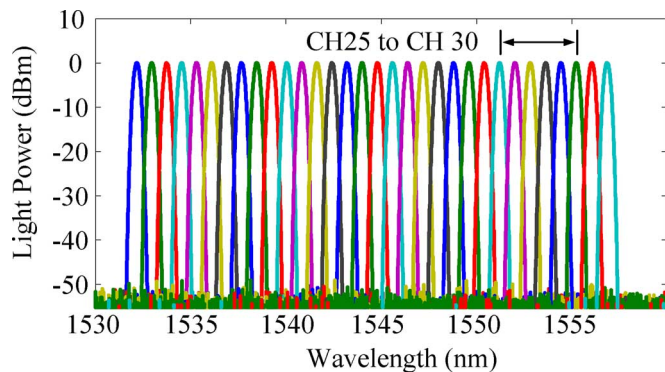


Fig. 1. Spectrum of the EDG having 32 channels, including odd and even number channels.

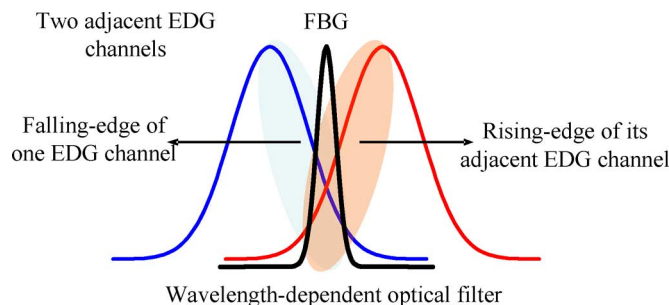


Fig. 2. Wavelength-dependent optical filter with two EDG channels.

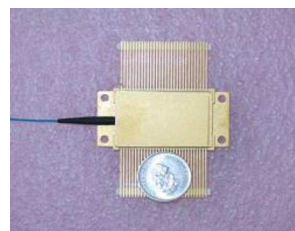


Fig. 3. Packaged EDG device.

interrogation of FBG acoustic sensors, which can be further implemented in the aerospace impact damage detection.

Therefore, the modified EDG interrogator can operate at both the sweeping mode and the parked mode, which can be used for the interrogation of FBG sensors for operational load monitoring and for impact damage detection.

## III. EXPERIMENTAL SETUP AND RESULTS

Fig. 3 shows the picture of the packaged EDG device used in this work. The device includes a  $1 \times 32$  EDG demultiplexer monolithically integrated with a detector array on an indium phosphide (InP) chip and is fabricated using semiconductor processing techniques [20].

The packaged EDG device has a weight of about 60 g and a dimension of  $45 \text{ mm} \times 30 \text{ mm} \times 15 \text{ mm}$ . It has 60 pins, including 32 pins connected to the detector array, 4 pins to the thermal electrical cooler (TEC) for the control of the EDG temperature, 4 pins to the resistance temperature detector (RTD) for the monitoring of the EDG temperature, and 2 pins for the +5 V power supply. Since the EDG channels are connected directly to the detector array, all the spectra of the EDG channels

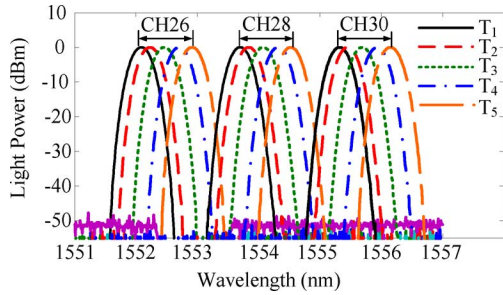


Fig. 4. Spectrum shift of the selected EDG channels versus temperature changes.

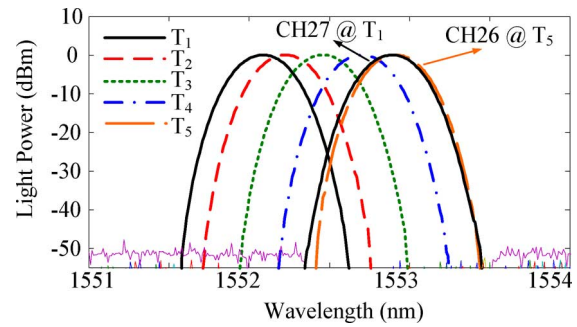


Fig. 6. Sweeping spectrum of CH 26 and the spectrum of CH 27 at the initial temperature.

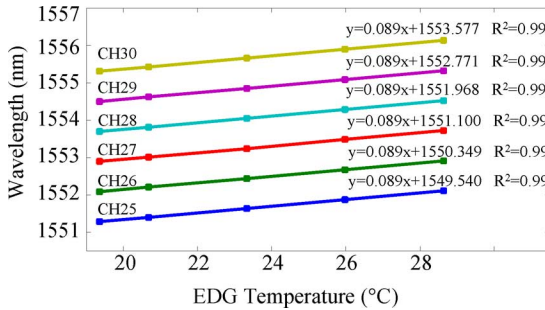


Fig. 5. Relationship between the transmission wavelength of each EDG channel and its temperature.

here are obtained by using an Agilent 8164B tunable laser with a sweeping step of 1 pm.

In this work, six EDG channels, from CH 25 to CH 30 (as labeled in Fig. 1), are used to perform the test, and the sweeping performance of the selected channels, CH 26, CH 28, and CH 30, are shown in Fig. 4.

Five discrete temperature values ( $T_1$  to  $T_5$ ) between  $19^\circ\text{C}$  to  $29^\circ\text{C}$  are chosen to test the sweeping spectrum of the modified EDG-based interrogator. It is seen that the sweeping spectrum profile of each channel keeps constant while the EDG temperature changes. The relationship between the transmission wavelength of each EDG channel and the temperature is also measured, which is used as a reference and shown in Fig. 5.

In Fig. 5, it is seen that all the EDG channels have the same spectrum sweeping capability in the modified EDG-based interrogator, which is similar to the results obtained in our previous studies [17], [18]. The sweeping coefficient is measured to be  $89 \text{ pm}/^\circ\text{C}$ . The use of all the 32 EDG channels makes the channel spacing be reduced from 1.6 nm to 0.8 nm, which also reduces the EDG temperature tuning range. In our previous studies, the EDG temperature needs to be tuned from  $20^\circ\text{C}$  to  $40^\circ\text{C}$  in order to achieve a 1.6-nm spectrum range for each EDG channel, which is used to cover the channel spacing and perform the full-spectrum sweeping. In this work, an EDG temperature tuning range of  $\sim 10^\circ\text{C}$  is enough for each EDG channel to cover the 0.8-nm channel spacing. Fig. 6 shows the sweeping spectrum of CH 26 at the five discrete temperature values and the spectrum of CH 27 at the initial temperature of  $19.36^\circ\text{C}$ .

It is seen that the spectrum of CH 26 at the temperature of  $28.63^\circ\text{C}$  has already exceeded the spectrum of CH 27 at the initial temperature of  $19.36^\circ\text{C}$ , which means that an EDG temperature tuning range from  $19.36^\circ\text{C}$  to  $28.63^\circ\text{C}$  is able to provide

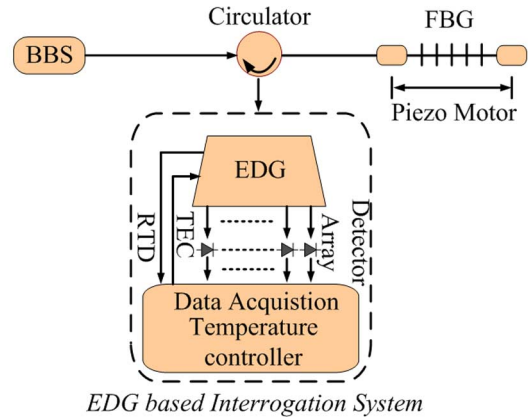


Fig. 7. Experimental setup of the proposed interrogation system.

a full-spectrum interrogation range. Compared with the temperature tuning range of  $\sim 20^\circ\text{C}$  in the previous work [17], [18], the power consumption is reduced. Furthermore, as described in [17], the measurement error could be decreased if a faster wavelength sweeping is applied. In this paper, the temperature tuning range is reduced by half, resulting in a smaller period in each sweeping cycle. Therefore, the measurement error could be decreased by using the modified EDG device.

The experimental setup is shown in Fig. 7. An FBG sensor is mounted on a closed-loop piezo motor, which is used to precisely apply a strain on the FBG sensor. A broadband source (BBS) is used as the light source. The reflected signal from the FBG sensor is then introduced into the proposed interrogation system. A LabView program is developed to perform the temperature control, light power acquisition, and data processing with a friendly user interface.

As discussed above, two operation modes are studied to confirm their potentials for operational load monitoring and impact damage detection. In the sweeping mode, the EDG temperature is tuned from  $19.36^\circ\text{C}$  to  $28.63^\circ\text{C}$ , which is achieved by changing the TEC control voltage from 1.055 V to 1.091 V. Within the 36 mV TEC tuning range, a step of 0.4 mV is applied, which is performed by the analog output function of a data acquisition card (National Instrument, DAQ PCI-6221). Thus, a temperature tuning step of  $0.1^\circ\text{C}$  is obtained, which makes a wavelength sweeping step as of 9 pm. During each temperature tuning step, the EDG temperature from the RTD is sampled by

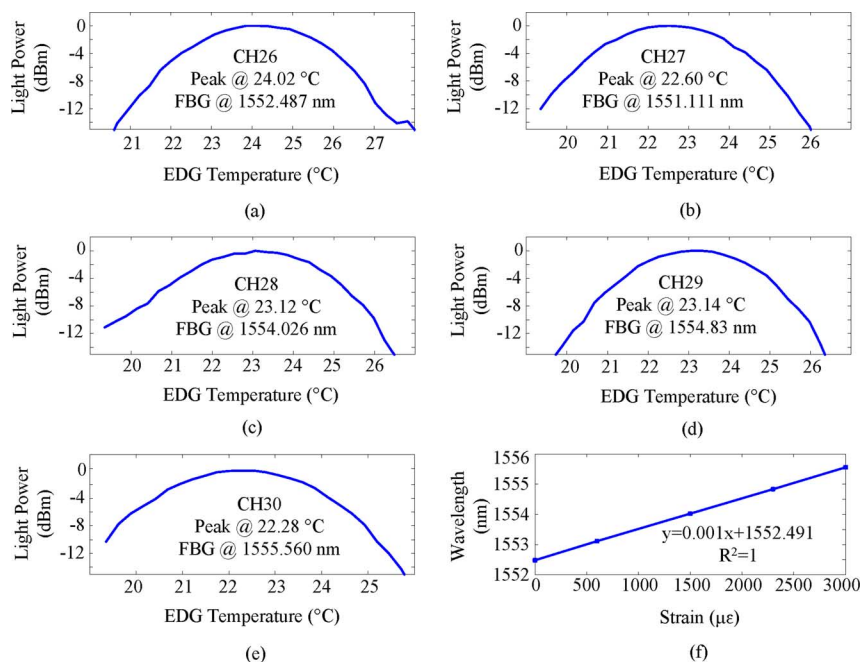


Fig. 8. Interrogation results of the FBG sensor under five different strains. (a)–(e) Light power with respect to the EDG temperature of the designated EDG channels. (f) Interrogated Bragg wavelength as a function of the strain applied.

another 10 measurement points, resulting in an estimated temperature change step of  $0.01^\circ\text{C}$ . Therefore, an accurate resolution of 9 pm is achieved based on the 0.4 mV voltage change. In addition, with the 10 more points to sample each temperature change step, we could get the smallest interrogation wavelength with an estimated value at 1 pm level, resulting in the final resolution in sub-pm level. Furthermore, a built-in peak searching function in the LabView program is applied to determine the temperature corresponding to the peak light power.

The interrogation of an FBG sensor under five different strains ( $0 \mu\epsilon$ ,  $600 \mu\epsilon$ ,  $1500 \mu\epsilon$ ,  $2300 \mu\epsilon$ , and  $3000 \mu\epsilon$ ) is demonstrated. Fig. 8(a)–(e) shows the light power with respect to the EDG temperature of the designated EDG channels. Each EDG channel has a measurement range of 0.8 nm, which is defined by the temperature tuning settings and the EDG channel spacing. Therefore, the Bragg peak positions of the FBG sensor corresponding to the five different strains are located within different EDG channels. The temperature representing the peak light power in each EDG channel is obtained by the built-in LabView peak searching function. By employing the reference shown in Fig. 5, we are able to calculate the Bragg wavelength of the FBG sensor under the five strains. Fig. 8(f) shows the relationship between the interrogated Bragg wavelength and the strain applied. It is seen that the Bragg wavelength increases with the strain at a rate of  $1 \text{ pm}/\mu\epsilon$ , which is typical for FBG sensors working at around 1550 nm [21]. Moreover, the repeatability of the proposed interrogation system prototype is also tested. In this test, a certain strain is constantly applied on the FBG sensor. For simplicity, three measurements are taken with a time interval of 5 minutes. The experimental result is shown in Fig. 9.

It is seen that better than 10-pm repeatability is achieved. As discussed above, the channel spacing is reduced from 1.6 nm to 0.8 nm in this work, resulting that the EDG temperature tuning

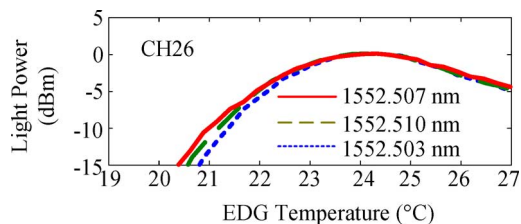


Fig. 9. Experimental result for the repeatability test.

range is from  $20^\circ\text{C}$  to  $30^\circ\text{C}$  rather than from  $20^\circ\text{C}$  to  $40^\circ\text{C}$  in our previous studies. By using the best operation range of the TEC, to avoid the use of higher temperature range, and to reduce the time period of each sweeping cycle, the repeatability is improved.

Next, the parked mode of the proposed interrogation system is tested. In the parked mode, the EDG spectrum is fixed by keeping the EDG temperature constant at  $30^\circ\text{C}$ , at which the TEC is tested to have the best performance. Due to the lack of an acoustic signal generator, the parked mode is tested by monitoring the movement of a piezo motor. In the parked mode, two adjacent EDG channels are used to function as a wavelength-dependent optical filter. The Bragg wavelength shifts are converted into the light power changes from the two channels. By monitoring the ratio of the light power from the two channels, the Bragg wavelength is measured [22]. The experimental result is shown in Fig. 10.

Two EDG channels, CH 27 and CH 28, are used in this test. Fig. 10(a) shows the light powers from the two channels while the piezo motor is moving, and Fig. 10(b) shows the ratio of the light powers, which could be used to reflect the Bragg wavelength shifts and the movement of the piezo motor. Based on the data processing methods in [16] and [22], the Bragg wavelength shift is measured to be from 1553.810 nm to 1554.290 nm. Thus,

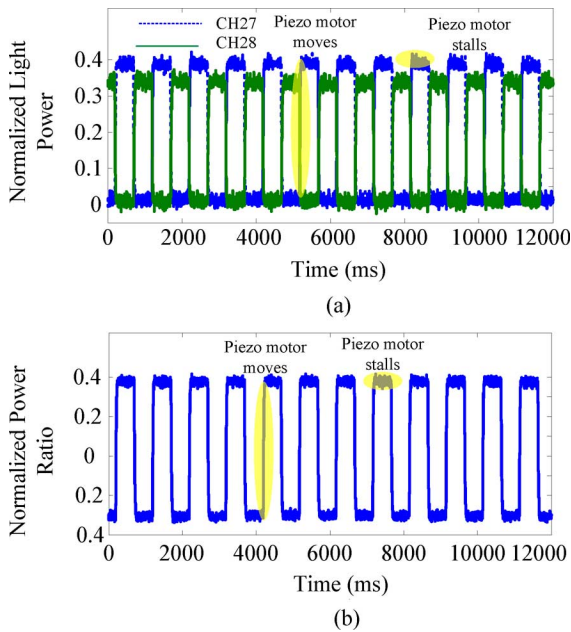


Fig. 10. Experimental result of monitoring the movement of a piezo motor. (a) Light power from two designated EDG channels. (b) Illustration of the movement.

when the piezo motor moves from one end to the other end, a strain of  $480 \mu\epsilon$  is applied to the FBG sensor. Considering the length of 42 cm between the two ends of the FBG sensor fixed on the stage, as shown in Fig. 7, the travel range of the piezo motor is measured to be  $200 \mu\text{m}$ . As shown in Fig. 10, the piezo motor takes 10 ms to travel from one end to the other. The measured piezo motor movement agrees well with the initial settings. Since the EDG has the same spectrum as an AWG as shown in Fig. 1 and a similar technique to achieve an interrogation speed of 300 kHz has been demonstrated in [16], the parked mode has a potential to reach an ultrafast speed for acoustic wave measurement in aerospace damage detection.

In the previous studies [16]–[22], the Bragg wavelength of the FBG sensor is required to be tuned at the middle between two adjacent channels before each measurement. This process introduces an additional calibration work. Although it could be achieved by shifting the EDG spectrum, it is not feasible for the use of multiplexed FBG sensors for real implementation, because each Bragg wavelength is independent and the calibration work for each sensor might not be the same. Considering that the parked mode is employed to eventually measure the acoustic waves for the impact damage detection, a maximum of three EDG channels is able to provide sufficiently large spectrum range, since the strain variation induced by the acoustic waves is within the range of hundreds or tens of  $\mu\epsilon$ . In this paper, the use of three EDG channels is demonstrated with the experimental result shown in Fig. 11.

Fig. 11 shows the first 1000 measurement points in the test. In Fig. 11(a), light power from three EDG channels, CH 26, CH 27, and CH 28, are illustrated. It is seen that Region 1 represents that the piezo motor stalls, and Regions 2 and 3 represent that the piezo motor moves. More specifically, Region 2 indicates that the Bragg wavelength shifts between CH 26 and CH 27, and the Bragg wavelength should be interrogated by using

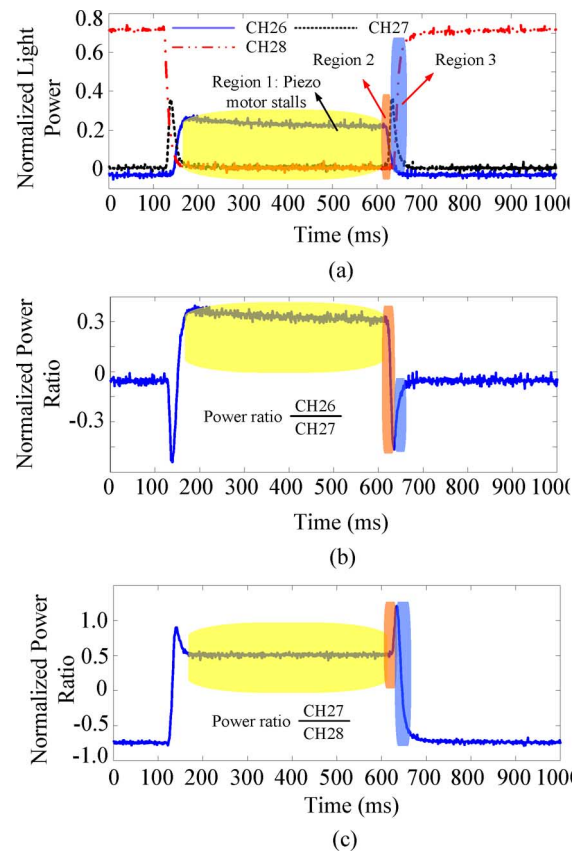


Fig. 11. Experimental result of using three EDG channels. (a) Light powers from the three channels. (b) Light power ratio between CH 26 and CH 27. (c) Light power ratio between CH 27 and CH 28.

the power ratio in Fig. 11(b). Region 3 indicates that the Bragg wavelength shifts between CH 27 and CH 28, and the power ratio in Fig. 11(c) is used to perform the wavelength interrogation. Similarly, the Bragg wavelength is measured to shift from 1553.135 nm to 1554.625 nm, and it represents that the travel range of the piezo motor is  $626 \mu\text{m}$ , which agrees well with the initial settings. Therefore, the effectiveness of the use of three EDG channels in the parked mode has been verified, and no additional calibration work, such as tuning the EDG spectrum, is required before each measurement.

The measurement error from this interrogator system is believed to be attributed to the broad bandwidth of the EDG channel and the power fluctuations, mainly from the broadband light source. Ideally, in the sweeping mode the EDG spectrum has a Dirac delta function profile with an infinite height and a unity area. In real implementation, however, the EDG spectrum has a 3-dB bandwidth of 0.4 nm, which is comparable or even larger than the bandwidth of the FBG sensor. Better accuracy could be achieved by reducing the EDG spectrum bandwidth. In the parked mode, the EDG spectrum bandwidth is tested to be proportional to the measurement resolution and error [22]. Thus, better results could be obtained by using an EDG with a smaller 3-dB bandwidth. The impact due to the power fluctuations on the measurement error mainly comes from the broadband light source. As discussed in [17], a fast wavelength tuning or the use of one EDG channel as the reference will alleviate this impact and a more accurate result could be obtained.

The proposed interrogation system is proven to have a small size and light weight, as shown in Fig. 3. In addition to the application for both operational load monitoring and impact damage detection, it also features low power consumption. The packaged EDG device is operated with a +5 V power supply, which can be powered by a battery. This feature allows the integration of energy harvesting techniques into the proposed interrogation system and makes it self-powered. Furthermore, a total of 32 EDG channels provide a capability to perform a multichannel interrogation for multiplexed FBG sensors, which is also a favorite feature for aerospace applications.

#### IV. CONCLUSION

An interrogation system based on an EDG for both operational load monitoring and impact damage detection with improved performance was proposed and experimentally demonstrated. Compared with our previous work, two improvements have been made. First, all the 32 EDG channels were used, resulting in a smaller temperature tuning range, faster speed, and better measurement repeatability. Second, two operation modes, the sweeping mode and the parked mode, were introduced. Especially, the use of three EDG channels in the parked mode was demonstrated. In the sweeping mode, the EDG spectrum was tuned by changing its temperature, which would provide a large measurement range at a low speed and was suitable for operational load monitoring. In the parked mode, the EDG spectrum was fixed by keeping its temperature a constant, in which two or three EDG channels were used to function as a wavelength-dependent optical filter for potential acoustic wave measurement. Preliminary results have verified the effective operations of the interrogator in two operation modes. Furthermore, the proposed interrogation system has the potential to be packaged into a palm-size, light-weight device with self-powered capability, which will make it ideal for aerospace applications.

#### REFERENCES

- [1] C. Boller, "Ways and options for aircraft structural health management," *Smart Mater. Struct.*, vol. 10, no. 3, pp. 432–439, 2001.
- [2] C. Boller and W. J. Staszewski, "Aircraft structural health and usage monitoring," in *Health Monitoring of Aerospace Structures*, W. Staszewski, C. Boller, and G. Tomlinson, Eds. New York, NY, USA: Wiley, 2003, pp. 29–73.
- [3] N. Aldridge, P. Foote, and I. Read, "Operational load monitoring for aircraft and maritime applications," *Strain*, vol. 36, no. 3, pp. 123–126, 2000.
- [4] P. Tua, S. Quek, and Q. Wang, "Detection of cracks in plates using piezo-actuated Lamb waves," *Smart Mater. Struct.*, vol. 13, no. 4, pp. 643–660, 2004.
- [5] E. Udd, "Review of multi-parameter fiber Bragg sensors," in *Proc. SPIE.*, 2007, vol. 6770, Paper 677002.
- [6] J. Lee, C. Ryu, B. Koo, S. Kang, C. Hong, and C. Kim, "In-flight health monitoring of a subscale wing using a fiber Bragg grating sensor system," *Smart Mater. Struct.*, vol. 12, no. 1, pp. 147–155, 2003.
- [7] M. Majumder, T. Gangopadhyay, A. Chakraborty, K. Dasgupta, and D. Bhattacharya, "Fibre Bragg gratings in structural health monitoring—Present status and applications," *Sensor Actuat. A*, vol. 147, no. 1, pp. 150–164, 2008.
- [8] K. Hill and G. Meltz, "Fiber Bragg grating technology fundamentals and overview," *J. Lightw. Technol.*, vol. 15, no. 8, pp. 1263–1276, Aug. 1997.
- [9] S. Grattan, S. Taylor, T. Sun, P. Basheer, and K. Grattan, "Monitoring of corrosion in structural reinforcing bars: Performance comparison using in situ fiber-optic and electric wire strain gauge systems," *IEEE Sens. J.*, vol. 9, no. 11, pp. 1494–1502, 2009.

- [10] D. Betz, G. Thursby, B. Culshaw, and W. Staszewski, "Identification of structural damage using multifunctional Bragg grating sensors: I. Theory and implementation," *Smart Mater. Struct.*, vol. 15, no. 5, pp. 1305–1312, 2006.
- [11] D. Betz, J. Staszewski, G. Thursby, and B. Culshaw, "Multi-functional fibre Bragg grating sensors for fatigue crack detection in metallic structures," *J. Aerospace Eng.*, vol. 220, no. 5, pp. 453–461, 2006.
- [12] B. Culshaw, G. Thursby, D. Betz, and B. Sorazu, "The detection of ultrasound using fiber-optic sensors," *IEEE Sens. J.*, vol. 8, no. 7, pp. 1360–1367, 2008.
- [13] A. Hongo, S. Kojima, and S. Komatsuzaki, "Applications of fiber Bragg grating sensors and high-speed interrogation techniques," *Struct. Contr. Health Monit.*, vol. 12, pp. 269–282, 2005.
- [14] M. Todd, J. Nichols, S. Trickey, M. Seaver, C. Nichols, and L. Vigin, "Bragg grating-based fibre optic sensors in structural health monitoring," *Phil. Trans. R. Soc. A*, vol. 365, no. 1851, pp. 317–343, 2007.
- [15] J. Frieden, J. Cugnoni, J. Botsis, T. Gmur, and D. Coric, "High-speed internal strain measurements in composite structures under dynamic load using embedded FBG sensors," *Compos. Struct.*, vol. 92, no. 8, pp. 1905–1912, 2010.
- [16] H. Soejima, T. Ogisu, H. Yoneda, Y. Okabe, N. Takeda, and Y. Koshioka, "Demonstration of detectability of SHM system with FBG/PZT hybrid system in composite wing box structure," in *Proc. SPIE*, 2008, vol. 6932, p. 69322E.
- [17] G. Xiao, N. Mrad, F. Wu, Z. Zhang, and F. Sun, "Miniaturized optical fiber sensor interrogation system employing echelle diffractive gratings demultiplexer for potential aerospace applications," *IEEE Sens. J.*, vol. 8, no. 7, pp. 1202–1207, 2008.
- [18] H. Guo, G. Xiao, N. Mrad, and J. Yao, "Simultaneous interrogation of a hybrid FBG/LPG sensor pair using a monolithically integrated echelle diffractive grating," *J. Lightw. Technol.*, vol. 27, no. 12, pp. 2100–2104, Dec. 2009.
- [19] Y. Sano and T. Yoshino, "Fast optical wavelength interrogator employing arrayed waveguide grating for distributed fiber Bragg grating sensors," *J. Lightw. Technol.*, vol. 21, no. 1, pp. 132–139, Jan. 2003.
- [20] V. Tolstikhin, A. Densmore, K. Pimenov, Y. Logvin, F. Wu, S. Laframboise, and S. Grachtchak, "Monolithically integrated optical channel monitor for DWDM transmission systems," *J. Lightw. Technol.*, vol. 17, no. 1, pp. 1710–1712, Jan. 2005.
- [21] Y. Rao, *Optical Fiber Sensor Technology*. London, U.K.: Chapman & Hall, 1998, ch. 2.
- [22] P. Cheben, E. Post, S. Janz, J. Albert, A. Laronce, J. H. Schmid, D. X. Xu, B. Jamontagne, J. Lapointe, A. Delage, and A. Densmore, "Tilted fiber Bragg grating sensor interrogation system using a high-resolution silicon-on-insulator arrayed waveguide grating," *Opt. Lett.*, vol. 33, no. 22, pp. 2647–2649, 2008.

**Honglei Guo** received the M.S. degree in optics from Nankai University (China) in 2006.

He is currently working toward the Ph.D. degree in the Microwave Photonics Research Laboratory, School of Electrical Engineering and Computer Science, University of Ottawa, Ottawa, ON, Canada. His current research interests include fiber optic sensors, sensor interrogation systems, micro and nano photonic fabrication, bio-photonics, and microwave photonics.

**Gaozhi (George) Xiao** received the Ph.D. degree from Loughborough University of Technology (UK) in 1995.

His experience ranges from industries to academics and covers the areas from materials to photonics. He was a R&D engineer and team leader in Chinese Aerospace Corporation from 1987 to 1992, a Research Fellow in Ecole Nationale Supérieure des Mines de Paris from 1995 to 1997, a R&D engineer in JDS Uniphase from 1998 to 1999, a senior product development engineer and a R&D group manager in Zenastra Photonics from 1999 to 2001, a senior product designer in Lumenon Innovative Lightwave Technology from 2001 to 2002. In April 2002 he joined the National Research Council (NRC) of Canada as a research scientist. He is currently a senior Research Officer in the Institute for Microstructural Sciences at NRC.

Dr. Xiao is a senior member of IEEE Instrumentation and Measurement Society, a steering committee member of IEEE/OSA Journal of Lightwave Technology. He is also an adjunct professor of Carleton University.

**Nezih Mrad** received his Ph.D. degree from The Pennsylvania State University (USA) in 1995.

He is currently an Operational Research Scientist at Centre for Security Science (CSS) of Defence R&D Canada of the Department of National Defence in Canada. His research work mainly focuses on the development of advanced technologies in support of military and aerospace platforms life extension and management.

**Jianping Yao** (M'99–SM'01–F'12) joined the School of Electrical Engineering and Computer Science, University of Ottawa, Ottawa, Ontario, Canada, as an Assistant Professor in 2001, where he became an Associate Professor in 2003, and a Full Professor in 2006. He was appointed University Research Chair in Microwave Photonics in 2007. From July 2007 to June 2010, he was the Director of the Ottawa-Carleton Institute for Electrical and Computer Engineering. Prior to joining the University of Ottawa, he was an Assistant Professor in the School of Electrical and Electronic Engineering, Nanyang Technological University, Singapore, from 1999 to 2011. He received the Ph.D. degree in electrical engineering from the Université de Toulon, Toulon, France, in December 1997.

Prof. Yao has published more than 400 papers, including more than 220 papers in peer-reviewed journals and 180 papers in conference proceedings. His research interests focus on microwave photonics, which includes photonic processing of microwave signals, photonic generation of microwave, millimeter-wave and terahertz, radio over fiber, ultrawideband over fiber, and photonic

generation of microwave arbitrary waveforms. His research also covers fiber optics and biophotonics, which includes fiber lasers, fiber and waveguide Bragg gratings, fiber-optic sensors, microfluidics, optical coherence tomography, and Fourier-transform spectroscopy. Dr. Yao is currently an Associate Editor of the International Journal of Microwave and Optical Technology. He is on the Editorial Board of the IEEE Transactions on Microwave Theory and Techniques. He is a Chair of numerous international conferences, symposia, and workshops, including the Vice Technical Program Committee (TPC) Chair of the IEEE Microwave Photonics Conference in 2007, TPC Co-Chair of the Asia-Pacific Microwave Photonics Conference in 2009 and 2010, TPC Chair of the high-speed and broadband wireless technologies subcommittee of the IEEE Radio Wireless Symposium in 2009–2012, TPC Chair of the microwave photonics subcommittee of the IEEE Photonics Society Annual Meeting in 2009, TPC Chair of the IEEE Microwave Photonics Conference in 2010, and General Co-Chair of the IEEE Microwave Photonics Conference in 2011. He is also a committee member of numerous international conferences. Prof. Yao received the 2005 International Creative Research Award of the University of Ottawa. He was the recipient of the 2007 George S. Glinski Award for Excellence in Research. In 2008, he was awarded a Natural Sciences and Engineering Research Council of Canada Discovery Accelerator Supplements Award. Prof. Yao was selected to receive an inaugural OSA Outstanding Reviewer Award in 2012. Currently, Prof. Yao serves as an IEEE Distinguished Microwave Lecturer for 2013–2015.

Prof. Yao is a registered Professional Engineer of Ontario. He is a Fellow of IEEE, a Fellow of the Optical Society of America (OSA), and a Fellow of the Canadian Academy of Engineering (CAE).